

Evaluation of composite membranes for direct methanol fuel cells

X. Li, E.P.L. Roberts*, S.M. Holmes

School of Chemical Engineering and Analytical Science, The University of Manchester, P.O. Box 88, Sackville Street, Manchester M60 1QD, UK

Received 19 October 2004; received in revised form 11 March 2005; accepted 14 March 2005

Available online 3 June 2005

Abstract

The performance of direct methanol fuel cells (DMFCs) can be significantly affected by the transport of methanol through the membrane, depolarising the cathode. In this paper, the literature on composite membranes that have been developed for reduction of methanol crossover in DMFCs is reviewed. While such membranes can be effective in reducing methanol permeability, this is usually combined with a reduction in proton conductivity. Measurements of methanol permeability and proton conductivity are relatively straightforward, and these parameters (or a membrane ‘selectivity’ based on the ratio between them) are often used to characterize DMFC membranes. However, we have carried out one-dimensional simulations of DMFC performance for a wide range of membrane properties, and the results indicate that DMFC performance is normally either limited by methanol permeability or proton conductivity. Thus use of a ‘selectivity’ is not appropriate for comparison of membrane materials, and results from the model can be used to compare different membranes. The results also show that Nafion® 117 has an optimum thickness, where DMFC performance is equally limited by both methanol permeability and proton conductivity. The model also indicates that new composite membranes based on Nafion® can only offer significant improvement in DMFC performance by enabling operation with increased methanol concentration in the fuel. A number of composite membrane materials that have been reported in the literature are shown to deliver significant reduction in DMFC performance due to reduced proton conductivity, although improved performance at high methanol concentration may be possible.

© 2005 Elsevier B.V. All rights reserved.

Keywords: Direct methanol fuel cell (DMFC); Membrane; Nafion®; Methanol crossover

1. Introduction

Ideally, the membrane in a direct methanol fuel cell (DMFC) should have high proton conductivity and low permeability for other species, particularly methanol. Nafion®, which is widely used in the PEM fuel cell, is a good proton conductor when it absorbs water but has a high methanol permeability due to: (a) active transport with protons and water; (b) diffusion through the water-filled pores within the Nafion®-structure; (c) diffusion through the Nafion® itself [1]. Active transport is thought to be the main mechanism for methanol permeation.

A number of approaches have been developed to reduce methanol crossover in DMFC membrane materials, including modification of Nafion® (e.g. by impregnation of

Pd nanoparticles [2] or silica [3], or by surface modification [4]); the use of alternative proton-conducting materials, particularly non-perfluorinated polymers (e.g. ZrO₂-SPEEK [5]); the use of composite polymer–zeolite materials (e.g. Nafion®–chabazite [6]).

Although a number of materials have been developed, it is difficult to determine which of these materials will offer the best DMFC performance. Fuel cell tests are of course desirable, but this approach can be expensive and difficult to reproduce due to the variability of the many factors which effect fuel cell performance (e.g. electrocatalysis, membrane electrode assembly fabrication, gas diffusion layer fabrication, flow distribution). A common approach has been to determine a ‘selectivity’ (for protons versus methanol) for each membrane based on measurements of the proton conductivity and methanol permeability [6–8]. However, it is not clear that a membrane with a higher selectivity will always give improved DMFC performance.

* Corresponding author. Tel.: +44 161 306 8849; fax: +44 161 306 4399.
E-mail address: edward.roberts@manchester.ac.uk (E.P.L. Roberts).

In this paper, we review the range of membrane materials that have been developed for reduced methanol crossover in DMFCs, and develop a model of DMFC performance to enable comparison of membrane materials based on their methanol permeability and proton conductivity.

2. Membrane materials for DMFCs

A wide range of membrane materials have been developed for reduced methanol crossover or improved proton conductivity in DMFCs. Details of many of these materials can be found in the detailed review of composite materials for medium temperature PEM fuel cells by Alberti and Casciola [9]. In this section, three categories of membrane materials are considered: (i) modified Nafion[®]; (ii) non-perfluorinated polymers; (iii) composite polymer–microporous silicate materials. Composite Nafion[®]–zeolite membranes, which could be considered under (i) or (iii), have been included in the latter category.

2.1. Modified Nafion[®]

Since Nafion[®] has excellent proton conductivity, a number of studies have attempted to modify Nafion[®] to reduce its methanol permeability. Kim et al. [2] impregnated a Pd nanophase into Nafion[®] 117 membranes. Compared to pure Nafion[®], this membrane material gave a seven-fold reduction in methanol permeability with only 35% reduction in proton conductivity. Fuel cell tests were carried out using both low (2 M CH₃OH) and high (10 M CH₃OH) concentrations of methanol. At low concentrations the Pd-modified membrane gave similar performance to the pure Nafion[®]. However, when the methanol concentration was increased the maximum power output of the fuel cell using pure Nafion[®] decreased by 43% while the cell using the Pd–Nafion[®] membrane gave an increase in maximum power output of 23%.

These results suggest that Pd-modified Nafion[®] may offer improved DMFC performance, although membrane cost may be an issue. Choi et al. [4] used surface modification, involving plasma etching and palladium sputtering on a Nafion[®] polymer membrane. Plasma etching of Nafion[®] membrane decreased the methanol permeability, possibly by reducing the pore size and increasing the hydrophobicity. The sputtering of palladium on the plasma-etched Nafion[®] further decreased the methanol crossover by pore plugging. The conductivity of the modified membranes was not determined. Although the methanol permeability was only slightly reduced (by around 33% overall), fuel cell tests indicated an increased open circuit voltage and increased power output. It seems likely that this improved performance may be due other effects, involving the modification of conditions at the reactant–electrocatalyst–electrolyte interface.

Dimitrova et al. [3] investigated recast Nafion[®]–silicon dioxide (Aerosil A380) composite membranes, with the objective of increasing the water uptake of Nafion[®] and thus

enhancing conductivity. It was found that Nafion[®]–silica powder membranes exhibited an increased water uptake and an associated three-fold increase in conductivity at 90 °C (compared with Nafion[®] 117). Similar methanol permeation rates to commercial Nafion[®] membrane were obtained. A similar composite membrane comprised of a mixture of tetraethylorthosilicate (TEOS) and Nafion[®] has been developed by Jung et al. [10], using an in situ sol–gel process. Although the water uptake of the Nafion[®] was enhanced, both the proton conductivity and the methanol permeability decreased, unlike the membrane developed by Dimitrova et al. [3].

Park et al. [11] have developed amorphous phosphate [di-isopropyl phosphate, HPO(OC₃H₇)₂]-Nafion[®] composite membranes. With increasing P/Nafion[®] ratio, the proton conductivity of the samples increased by up to 10 times. However, the membranes were found to be unstable.

In summary, a range of Nafion[®]-modified membrane materials has been developed. Of these, the incorporation of metal nanoparticles into the membrane offered the best performance in terms of reduced methanol crossover, while a silicon dioxide–Nafion[®] composite membrane exhibited significantly improved proton conductivity. An alternative PTFE based membrane material has been developed by Yamaguchi et al. [12]. This membrane consisted of a polyvinyl-sulfonic/acrylic acid cross-linked gel in a porous PTFE substrate. The results indicated that the substrate matrix effectively suppressed membrane swelling, resulting in lower methanol permeability, around 10 times less than that of Nafion[®]. Unfortunately, the proton conductivity also reduced to around half of the value of Nafion[®].

2.2. Non-perfluorinated polymers

There has been widespread interest in the development of low-cost non-perfluorinated proton-conducting polymers for fuel cell applications. Researchers at the GKSS Research Centre in Germany have developed a sulfonated polyether ether ketone (SPEEK) modified by in situ generation of SiO₂, TiO₂ or ZrO₂ to reduce methanol permeability [5,13]. They found that modification with ZrO₂ could lead to a 60-fold reduction of the methanol flux, however, a 13-fold reduction of conductivity was also observed. A good balance of high conductivity and low water and methanol permeability was possible when a mixture of ZrO₂ and zirconium phosphate was used. In this case, a 28-fold reduction of water flux was observed with only 10–30% reduction of proton conductivity.

Jung et al. [14] blended tetraethylorthosilicate with sulfonated styrene–(ethylene–butylene)–sulfonated styrene (SEBSS) to produce a composite membrane. The methanol permeability of the membrane was reduced by the addition of the TEOS, but if too much silica was added to the SEBSS membrane, the performance of a DMFC was affected due to a decrease in the proton conductivity.

A series of organic–inorganic composite materials based on polyethylene glycol (PEG)–SiO₂ has been evaluated by

Chang and Lin [15]. The hybrid materials were found to have reasonable proton conductivity (in the range 10^{-3} to 10^{-2} S cm $^{-1}$, around one order of magnitude less than Nafion $^{\text{®}}$) while their methanol permeability was about two orders of magnitude lower than that of Nafion $^{\text{®}}$ membrane for similar experimental conditions.

Sulfonated polyimide (SPI) membranes for DMFC have been synthesized by Woo et al. [16]. The proton conductivity of these membranes increased with the level of sulfonation up to around 4×10^{-2} S cm $^{-1}$ (similar to the conductivity of Nafion $^{\text{®}}$), while the methanol permeability was two to four orders of magnitude lower than that of Nafion $^{\text{®}}$.

One of the most widely studied polymers for DMFC is polybenzimidazole (PBI), which is a low cost, non-perfluorinated polymer [17]. As a polymer electrolyte for the DMFC, phosphoric acid doped PBI offers several advantages over Nafion $^{\text{®}}$, in particular good proton conductivity at temperatures above 150 °C. The conductivity of phosphoric acid doped PBI membrane material has been found to be around 4×10^{-2} S cm $^{-1}$ at 190 °C [18]. PBI based fuel cells can be operated at high temperature and low gas humidification without dehydrating the membrane, which could cause severe problems for Nafion $^{\text{®}}$, which loses its conductivity when dehydrated.

A range of promising non-perfluorinated membrane materials have been developed which offer reduced methanol permeability with reasonable proton conductivity. The durability of these materials in fuel cell environments will need to be demonstrated.

2.3. Composites of ion-conducting polymers and micro- or mesoporous silicates

To hinder permeation of methanol, one approach has been to develop composite membranes using zeolites, which have ‘molecular sieve’ properties due to their three-dimensional framework structures. The approach of most studies has been to take advantage of this molecular sieving property of zeolite to prevent methanol (which has a relatively large molecular size) from passing through the membrane. However, a pure zeolite exhibits poor mechanical properties such as brittleness and fragility and hence is unsuitable for use as a membrane [19]. When zeolite particles are combined with a polymer support (e.g. Nafion $^{\text{®}}$, PVA), the flexibility of the polymer makes the polymer–zeolite composite membrane an appealing solution, combining the advantages of both polymer and zeolite. Unfortunately, although the addition of zeolite can significantly reduce the methanol crossover, in most cases the proton conductivity is also decreased, because most zeolites without modification do not have high conductivity.

A zeolite-modified Nafion $^{\text{®}}$ membrane has been developed by Tricoli and Nannetti [6]. They used chabazite and clinoptilolite, which are chemically stable in aqueous solution within the pH range 3–12. The high silica (Si/Al \geq 4) clinoptilolite has a monoclinic layered structure with a two-

dimensional system of channels with mean diameters ranging from 3.5 to 5.0 Å. Chabazite, with Si/Al \geq 2, has a three-dimensional channel system with a minimum aperture of 3.8 Å. In principle, these materials should be size selective for water over methanol, which have critical dimensions of 3.2 and 4.4 Å, respectively. Unfortunately, Tricoli and Nannetti [6] found that the methanol permeability of the Nafion $^{\text{®}}$ was not substantially reduced by the presence of the zeolite, while the proton conductivity was significantly inferior. The composite membranes gave poor selectivity for protons when compared to recast Nafion $^{\text{®}}$. The authors took these results to indicate that while these zeolites were unsuitable, effective composite membranes could be developed by use of suitably selective zeolites. In a slightly different approach, a composite montmorillonite (MMT) Nafion $^{\text{®}}$ membrane has been fabricated by Jung et al. [20]. The membrane obtained showed an improved performance, but only at high operating temperature (e.g. 125 °C).

Cussler and co-workers [8,21] have developed a composite membrane based on polyvinylalcohol (PVA) and mordenite particles. Mordenite is stable up to temperatures above 800 °C [22], and in view of the mechanical properties of the membrane, PVA is a logical choice because it can be easily formed into a membrane, and has a permeability that can be altered thermally [8]. Because stability increases and hydrophilicity decreases as the SiO $_2$ /Al $_2$ O $_3$ ratio increases from 1 to ∞ , to obtain a compromise, Libby et al. [8,21] did not use the natural mordenite, which has a Si/Al ratio of 5; instead, they used a dealuminated form of mordenite with a SiO $_2$ /Al $_2$ O $_3$ ratio of 40. The results showed that the methanol permeability of the membrane was significantly lower than that of Nafion $^{\text{®}}$. With respect to the proton conductivity, the high conductivity of the acid doped mordenite counteracts the low polymer conductivity, resulting in around 10 times reduction in the proton conductivity of the composite. However, a significant increase in selectivity was obtained for these membranes compared to Nafion $^{\text{®}}$.

A composite membrane comprised of SPEEK, Laponite and MMT has been developed by Chang et al. [23]. SPEEK was chosen because of its good mechanical properties and good thermal and chemical stability. Laponite and MMT play a role in reducing methanol permeability and in addition could prevent excessive swelling at high temperature, a significant problem for DMFC membrane. The proton conductivity of the SPEEK membrane with 10 wt.% Laponite was around one-third of that of Nafion $^{\text{®}}$ membrane under the same conditions. The methanol permeability of this membrane was around one-quarter of that of Nafion $^{\text{®}}$, so that the selectivity of the membrane material is only slightly better than Nafion $^{\text{®}}$.

Poltarzewski et al. [24] synthesized a novel membrane by dispersing Zeolon 100H (the protonated form of mordenite) in PTFE. As PTFE is highly hydrophobic, the Zeolon particles take full responsibility for proton transport and the conductivity increased with an increase in the zeolite concentration. To achieve good conductivity, composite membranes

with up to 90 wt.% Zeolon were used. The high concentration of Zeolon led to a material with low tensile strength.

In summary, it would appear that there is only limited evidence for transport of protons through the zeolite structure in microporous silicate–polymer composites. The reduction in the methanol crossover may in the main be due to filling of the polymer with an organophobic structure (high alumina zeolites and clays) and there has been no evidence of enhanced or even equivalent proton conductivity to pure Nafion[®]. The only way to ensure that the molecular sieving properties of the zeolite are utilized is to form a coherent layer (membrane) of the target zeolite and select a hydrophilic structure, which will preferentially transport protons. However, the results obtained by Aricò et al. [25] show that the proton conductivity of Nafion[®] can be enhanced at elevated temperatures (up to 145 °C) using inorganic fillers. They found that the more acidic the filler surface, the better the enhancement of proton conductivity. A similar approach, using an inorganic power–PVDF gel composite, has been developed by Peled et al. [26,27]. These materials consist of a nanosize inorganic powder (such as silica, zirconia, titania or alumina which have a good retention capability for aqueous acids) combined with a PVDF or PAN [28] polymer binder. Proton conductivity is provided by an aqueous acid or mixture of acids, which fill the nanopores of the material. These materials are reported to offer increased proton conductivity (of order 0.01–0.2 S cm⁻¹) and reduced methanol permeability [27–29].

3. Modelling of fuel cell performance

As has been discussed previously, a good DMFC membrane should have high proton conductivity and low methanol permeability. The search for new membranes should begin by establishing the criteria for comparison of newly developed membrane with the benchmark of Nafion[®]. In many cases, a ‘selectivity’ for protons versus methanol has been used as an indicator of membrane performance [6,8,21]. However, an improved selectivity may not guarantee improved fuel cell performance. For example, a material with higher selectivity but lower conductivity may give lower fuel cell performance in practice. In this section, a model of DMFC performance (which includes the effects of membrane conductivity and methanol permeability) is developed in order to enable direct comparison of alternative membrane materials.

The model, based on that developed by Kulikovskiy [30,31], makes the following major assumptions:

- (i) The temperature is uniform throughout the cell.
- (ii) Ohmic voltage drop in the cell is caused by the membrane resistance only.
- (iii) Electrode kinetics are described by the Tafel equation.
- (iv) The methanol concentration in the anode catalyst layer is constant.
- (v) The oxygen pressure in the cathode catalyst layer is constant.

- (vi) The effect of electroosmosis on the rate of methanol transport through the membrane is negligible.
- (vii) For the purposes of determining the rate of transport of methanol across the membrane, the methanol concentration in the cathode catalyst layer is negligible compared to the concentration in the anode catalyst layer.
- (viii) The methanol concentration varies linearly in the membrane.
- (ix) The reactions at the anode and cathode are first order.
- (x) The concentration distributions are one-dimensional (i.e. concentration variations along and across the fuel cell are assumed to be negligible).

The overall voltage of a DMFC is given by:

$$U = E^0 - \eta_a - \eta_c - \eta_\Omega \quad (1)$$

where E^0 is the thermodynamic potential of a DMFC (taken to be 1.21 V), η_a and η_c the overpotential at the anode and cathode, respectively, and η_Ω is the ohmic potential drop in the cell.

Although the kinetics of oxygen reduction are Tafel like, methanol reduction is known to exhibit non-Tafel behaviour [32]. However, most models of DMFCs assume Tafel kinetics at the anode [30,31,33,34] and this is considered to be a reasonable first order approximation for the purposes of the model used here. The anode overpotential (η_a) is considered to include three terms associated with electron transfer, mass transport and the loss of methanol through the membrane:

$$\eta_a = b_a \ln \left(\frac{i}{i_{oa}} \right) - b_a \ln \left(1 - \frac{i}{i_{la}} \right) + b_a \ln(1 + \mu) \quad (2)$$

where b_a is anode Tafel slope, i the applied current density, i_{oa} the exchange current density at the anode, i_{la} the limiting current density at the anode and μ is the dimensionless parameter related to the properties of the backing layer and membrane [31]:

$$\mu = \frac{\beta L_{ba}}{L D_{ba}} \quad (3)$$

where β is the methanol permeability of the membrane, L the membrane thickness, L_{ba} the thickness of the anode backing layer and D_{ba} is the effective diffusivity of methanol in the backing layer.

The overpotential at the cathode includes contributions from electron transfer activation overpotential, mass transport and the consumption of oxygen due to reaction with methanol:

$$\eta_c = b_c \ln \left(\frac{i}{i_{oc}} \right) - b_c \ln \left(1 - \frac{i}{i_{lc}} - R_c \right) \quad (4)$$

where b_c is the cathode Tafel slope, i_{lc} the exchange current density at the cathode and R_c is the dimensionless parameter

associated with methanol crossover, given by:

$$R_c = \frac{i_{la}}{i_{lc}} \left(\frac{\mu}{1 + \mu} \right) \left(1 - \frac{i}{i_{la}} \right) \quad (5)$$

This equation is based on diffusional transport of methanol through the membrane and neglects the effect of electroosmosis [30,31]. The effect of electroosmosis is small for low methanol concentrations and current densities, and future refinement of the model may require the inclusion of electroosmosis effects.

Calculating the ohmic potential drop in the membrane as:

$$\eta_{\Omega} = \frac{iL}{\sigma} \quad (6)$$

where σ is the proton conductivity of the membrane, the cell voltage can thus be obtained by substituting equations (2)–(6) into equation (1).

Typical data from the literature [30,31,35–38] are used for the exchange current densities and Tafel slopes for the anode and cathode of a DMFC operating at 90 °C using a 1 M methanol solution:

$$i_{oa} = 131.6 \text{ A m}^{-2} \quad (7)$$

$$i_{oc} = 0.0839 \text{ A m}^{-2} \quad (8)$$

$$b_a = \frac{RT}{0.8F} \quad (9)$$

$$b_c = \frac{RT}{0.7F} \quad (10)$$

If necessary, the effect of temperature on the electrode kinetics can be included using data from Parthasarathy et al. [35] and Wang and Wang [38].

Following Kulikovskiy [30], the limiting current density at each electrode can be estimated from the properties of the backing layer and the methanol concentration:

$$i_{la} = 6F \frac{D_{ba} C_m}{L_{ba}} \quad (11)$$

$$i_{lc} = 4F \frac{D_{bc} C_o}{L_{bc}} \quad (12)$$

where F is Faraday's constant, D_{ba} the diffusion coefficient of methanol in the anode backing layer, D_{bc} the diffusion coefficient of oxygen in the cathode backing layer C_m and C_o are the concentration of methanol and oxygen at the feed

fuel and oxygen/air supply, and L_{ba} and L_{bc} are the thickness of backing layer at the anode and cathode. Typical parameter values for the backing layers in a DMFC operating at 90 °C are taken from Kulikovskiy [30], which were fitted to experimental data obtained by Sundmacher and Scott [39], as follows:

$$L_{ba} = L_{bc} = 0.3 \text{ mm} \quad (13)$$

$$D_{ba} = 1.8 \times 10^{-9} \text{ m}^2 \text{ s}^{-1} \quad (14)$$

$$D_{bc} = 9 \times 10^{-8} \text{ m}^2 \text{ s}^{-1} \quad (15)$$

Using the equations above, the cell potential (and thus the power output) of a DMFC can be calculated for any given current density, provided the membrane properties (thickness, L , proton conductivity, σ , and methanol permeability, β) and methanol concentration are specified. The power output of the DMFC can then be determined from the cell potential and applied current:

$$P = (E^o - \eta_a - \eta_c - \eta_{\Omega})i \quad (16)$$

The performance of a DMFC can be characterized by the maximum power output (P_{mx}), which can be determined numerically by varying i in equation (16). Note that the data for the anodic exchange current density [equation (7)] are for a 1 M methanol solution, and these must be adjusted when the methanol concentration is varied.

4. Evaluation of membrane materials

Three membrane materials reported in the literature are compared using the DMFC model described above. These include Nafion® 117, a sulfonated polyimide membrane [16], and a composite PVA–mordenite material [8]. Membrane thickness, proton conductivity and methanol permeability data from the literature for each of the selected materials is shown in Table 1.

For each membrane the DMFC output power density was determined as a function of current density using equation (16). The results obtained are plotted in Fig. 1, and the corresponding maximum power output is shown in Table 1. It is clear that the Nafion® membrane gives the best performance, with the composite PVA–mordenite a slightly lower power output and the SPI membrane giving very poor performance.

Table 1

Physical properties (thickness, L , proton conductivity, σ , and methanol permeability, β) of Nafion® 117, sulfonated polyimide (SPI) and PVA–mordenite (50%, v/v) DMFC membrane materials

| Membrane material | L (μm) | σ (S cm^{-1}) | β ($\text{cm}^2 \text{ s}^{-1}$) | s (S s cm^{-3}) | P_{mx} (W m^{-2}) | |
|-------------------|-----------------------|---------------------------------|--|------------------------------|--------------------------------|------|
| | | | | | 1 M | 10 M |
| Nafion® 117 | 175 | 0.1056 | 2.38×10^{-6} | 1.0 | 874 | – |
| SPI | 89 | 1.72×10^{-3} | 8.52×10^{-10} | 45 | 253 | 316 |
| PVA–mordenite | 100 | 0.012 | 1.25×10^{-8} | 22 | 747 | 951 |

The selectivity (σ/β) relative to Nafion® (s), and the calculated maximum power output (P_{mx}) for a DMFC using both 1 M and 10 M methanol solutions (Fig. 1) are also given.

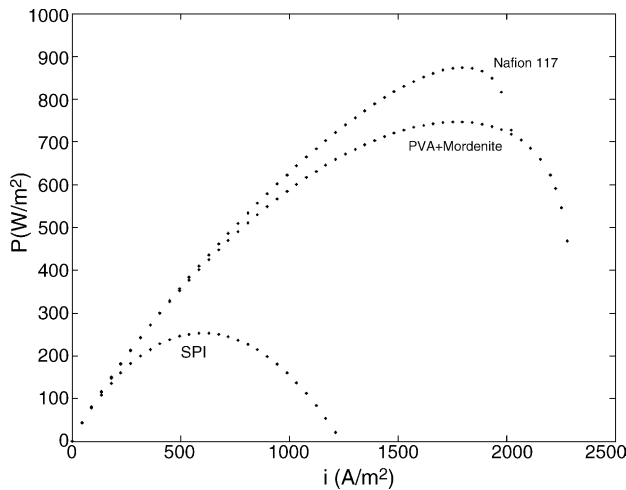


Fig. 1. Power density as a function of current density for a DMFC operating with a 1 M methanol fuel and three different membrane materials (Table 1). The power density was calculated using the model described in Section 3.

The results shown in Table 1 clearly show that selectivity (σ/β) is not a good indicator of membrane performance.

In order to provide a more general protocol for comparing membrane materials based on their proton conductivity and methanol permeability, the maximum DMFC power output has been calculated for a wide range of membrane material properties. The results obtained (Fig. 2) can be used to compare membrane materials directly based on the maximum DMFC power output. The results shown in Fig. 2 also show why the selectivity is not a good measure of membrane performance for DMFC applications. For membranes with low proton conductivity and low methanol permeability [$(\beta/L) < 10^{-6} \text{ cm}^2 \text{ s}^{-1}$], the maximum power

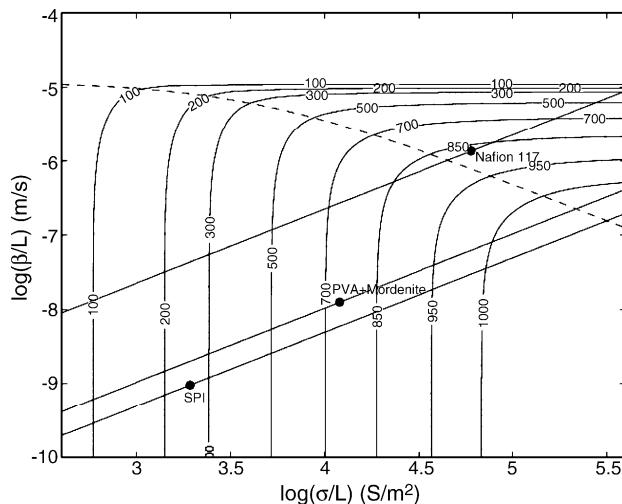


Fig. 2. Maximum power density (W m^{-2}) for a DMFC fuel cell as a function of the properties of the membrane material, for a 1 M methanol solution. Three membrane materials from the literature are plotted (see Table 1), along with lines indicating the effect of varying membrane thickness at constant β and σ . The dashed line corresponds to equation (20), which estimates conditions where the fuel cell is equally limited by membrane resistance and methanol crossover.

output is independent of β/L . This indicates that for these conditions, the DMFC performance is limited by the ohmic resistance of the cell, and reduction of methanol permeability will not improve cell performance, even when it increases selectivity. Conversely, for membranes with high proton conductivity and high methanol permeability, the DMFC power output is limited by methanol crossover. For methanol permeability greater than 10^{-5} m s^{-1} , the maximum power output rapidly falls to zero due to methanol crossover.

For the parameters used in Fig. 2, approximate solutions for P_{mx} for the extremes of ‘ohmic limited’ and ‘permeability limited’ conditions have been determined as follows (see Appendix A):

$$\text{Ohmic limited, } P_{\text{mx}} \approx \frac{0.25}{L/\sigma + (0.5 + b_c)/i_{\text{lc}}} \quad (17)$$

$$\text{Permeability limited, } P_{\text{mx}} \approx \frac{0.25(1 - \alpha)i_{\text{lc}}i_{\text{la}}}{(0.5 + b_c)(i_{\text{la}} - \alpha i_{\text{lc}})} \quad (18)$$

where

$$\alpha = \frac{i_{\text{la}}}{i_{\text{lc}}} \left(\frac{\mu}{1 + \mu} \right) \quad (19)$$

These approximations were found to be in good agreement with the numerical solutions obtained using the full model under appropriate conditions (i.e. small σ/L and β/L for ohmic limited and large σ/L and β/L for permeability limited), as shown in Fig. 3. For ohmic limited conditions, equation (17) slightly overestimates P_{mx} at intermediate values of σ/L , but for permeability limited conditions the agreement is excellent. As the permeability increases, the value of α increases. According to equation (18), once $\alpha = 1$ the maximum power output drops to zero, consistent with Fig. 2.

Variations in membrane thickness are considered by plotting the line corresponding to varying thickness (with constant β and σ) on the β/L versus σ/L figure. For the three materials studied, the effect of varying membrane thickness is shown in Fig. 2. Interestingly, Nafion[®] 117 was found to be close to its optimum thickness, while the performance of the SPI and PVA–mordenite membranes could be significantly improved with decreasing thickness. For both of SPI and PVA–mordenite power densities of 900 W m^{-2} (i.e. higher than what Nafion[®] 117) are achievable, but the required membrane thickness would be around 7 and $48 \mu\text{m}$, respectively. Fabrication of a membrane of $7 \mu\text{m}$ thickness would be impractical, while preparing a robust composite membrane with a thickness of $48 \mu\text{m}$ could be a significant challenge, depending on the particle size used.

The position of the point of optimum thickness on the lines plotted in Fig. 2 corresponds to the boundary between ohmic limited and permeability limited conditions. The location of the line separating these two conditions can be estimated using equations (17) and (18), by equating the maximum power output obtained in each case.

$$\frac{\sigma}{L} = \frac{i_{\text{lc}}i_{\text{la}}(1 - \alpha)}{\alpha(0.5 + b_c)(i_{\text{la}} - i_{\text{lc}})} \quad (20)$$

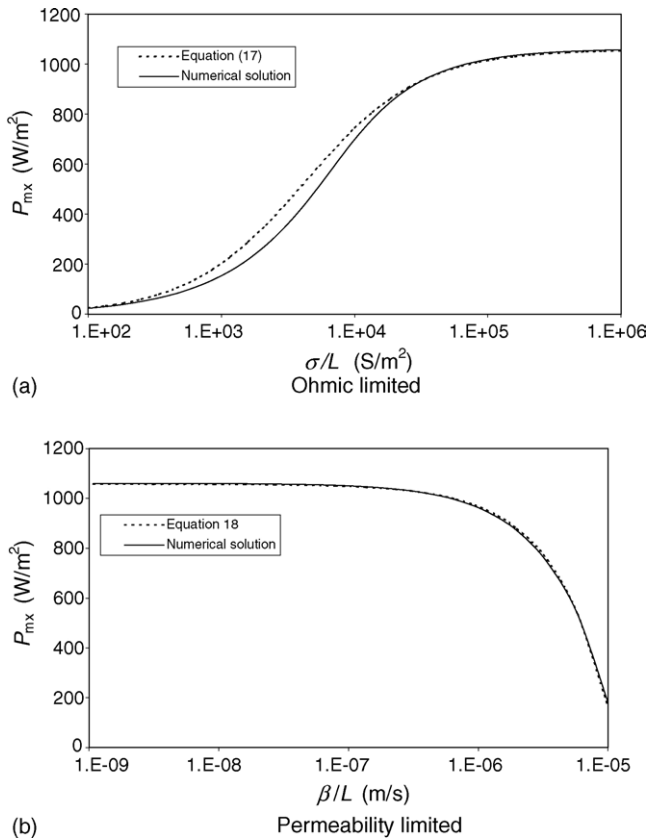


Fig. 3. The maximum fuel cell power under ohmic (a) and permeability (b) limited conditions. The full line shows the accurate numerical solution while the dotted line shows the approximate value determined using equations (17) and (18).

This line is plotted in Fig. 2, and clearly separates the two regimes. Equation (20) can be used to determine whether a membrane is ohmic or permeability limited; if the value of σ/L for a membrane is less than the right hand side of equation (20), then a fuel cell using this membrane will be ohmic limited and vice versa.

At high proton conductivities the DMFC performance reaches a maximum of around 1100 W m⁻², where performance is limited by mass transport overpotentials. A reduction in the methanol permeability of Nafion® 117 would clearly increase DMFC power output, but the improvement in performance would be relatively limited. Another approach to increasing power output is to increase the methanol fuel concentration. However, Kulikovsky [30] showed that for Nafion® 117, if the methanol concentration is above 0.97 M the performance decreases due to methanol crossover. With increased methanol concentration, the limiting methanol permeability ($\sim 10^{-6}$ cm² s⁻¹ for 1 M methanol, Fig. 2) where the fuel cell becomes proton conduction limited would be expected to decrease. Thus, the optimum methanol concentration when the power output is on the boundary between methanol limited and proton conduction limited conditions. Thus, the position of the Nafion® 117 data point in Fig. 2

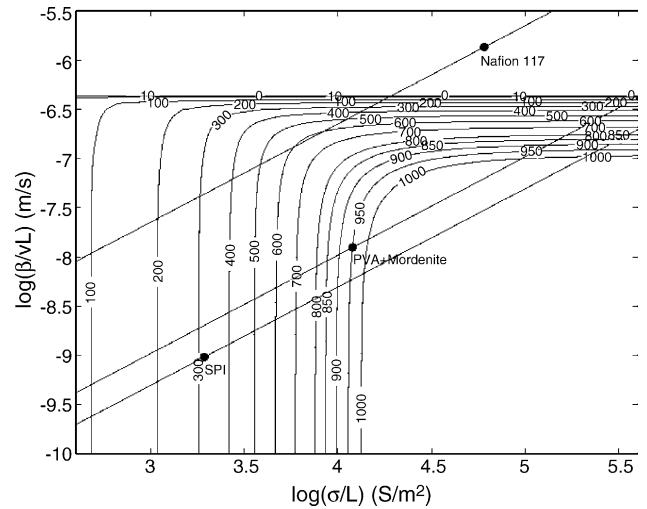


Fig. 4. Maximum power density for a DMFC fuel cell operating as a function of the properties of the membrane material, for a 10 M methanol solution. Three membrane materials from the literature are plotted (see Table 1), along with lines indicating the effect of varying membrane thickness at constant β and σ .

for 1 M methanol is consistent with the optimum found by Kulikovsky [30].

Fig. 4 shows the results obtained when the methanol concentration in the fuel was increased to 10 M. The power output for the Nafion® 117 is not specified, as the methanol crossover is so high that the fuel cell becomes fully depolarized and no power can be obtained. However, for both the SPI and the PVA–mordenite membrane the maximum power output is significantly increased (Table 1). In the case of the PVA–mordenite composite membrane, around 950 W m⁻² is obtained, better than for the Nafion® 117 under optimum conditions. However, the maximum power output at high proton conductivity and low methanol permeability remains around 1100 W m⁻², due to the limiting overpotentials at the cathode.

5. Concluding remarks

Libby et al. [8] pointed out that it may be essential to separate the mechanism of proton transport and methanol diffusion to improve membrane performance. Possible approaches for composite membranes include the use of zeolites containing proton conducting species (e.g. tin, ammonia [40]), or soaking membranes with an ionic liquid [41], which could take responsibility for proton transport.

It is clear that reducing methanol crossover in DMFCs may give improved fuel cell performance. However, most membrane materials, which have reduced methanol crossover also have low proton conductivity. The data published in this paper can be used to determine how these two factors effect fuel cell performance. While other factors such as durability and cost are important, the simple one-dimensional model of Kulikovsky [30,31] can be used to give a rapid comparison of candidate materials. Other parameters, including catalyst per-

formance (through the exchange current density) and diffusion layer thickness, could also be evaluated using the model.

Appendix A

The current density at P_{mx} is determined by differentiating equation (16):

$$\frac{dP}{di} = U - i \left(\frac{d\eta_a}{di} + \frac{d\eta_c}{di} + \frac{d\eta_\Omega}{di} \right) = 0, \quad \text{at } P_{\text{mx}} \quad (\text{A.1})$$

Taking $U \approx 0.5 \text{ V}$ at P_{mx} :

$$i = \frac{0.5}{\frac{d\eta_a}{di} + \frac{d\eta_c}{di} + \frac{d\eta_\Omega}{di}}, \quad \text{at } P_{\text{mx}} \quad (\text{A.2})$$

and

$$P_{\text{mx}} = \frac{0.25}{\frac{d\eta_a}{di} + \frac{d\eta_c}{di} + \frac{d\eta_\Omega}{di}} \quad (\text{A.3})$$

It was found that the activation overpotential terms had little effect on the current density at maximum power.

A.1. Ohmic limited conditions

Neglecting the activation overpotential terms and putting $\beta = 0$, equations (2), (4) and (6) become:

$$\eta_a = -b_a \ln \left(1 - \frac{i}{i_{\text{la}}} \right) \quad (\text{A.4})$$

$$\eta_c = -b_c \ln \left(1 - \frac{i}{i_{\text{lc}}} \right) \quad (\text{A.5})$$

$$\eta_\Omega = \frac{iL}{\sigma} \quad (\text{A.6})$$

Differentiating equations (A.4)–(A.6) we obtain:

$$\frac{d\eta_a}{di} = \frac{b_a}{i_{\text{la}} - i} \quad (\text{A.7})$$

$$\frac{d\eta_c}{di} = \frac{b_c}{i_{\text{lc}} - i} \quad (\text{A.8})$$

$$\frac{d\eta_\Omega}{di} = \frac{L}{\sigma} \quad (\text{A.9})$$

Equations (A.7) and (A.8) correspond to mass transport limiting overpotentials. Since $i_{\text{la}} > i_{\text{lc}}$, the cell will limit on cathodic mass transport and the anodic term can be neglected. For cathodic mass transport limiting conditions, $\frac{d\eta_\Omega}{di} \ll \frac{d\eta_c}{di}$, substituting (A.8) into equation (A.2) and rearranging we obtain:

$$i = \frac{0.5i_{\text{lc}}}{b_c + 0.5} \quad (\text{A.10})$$

Substituting this back into equation (A.8):

$$\frac{d\eta_c}{di} = \frac{0.5 + b_c}{i_{\text{lc}}} \quad (\text{A.11})$$

Substituting (A.9) and (A.11) into equation (A.3) for ohmic limited conditions we obtain:

$$P_{\text{mx}} \approx \frac{0.25}{L/\sigma + (0.5 + b_c)/i_{\text{lc}}} \quad (\text{A.12})$$

A.2. Permeability limited conditions

Neglecting the activation overpotential terms and putting $L/\sigma = 0$ for permeability limited conditions, equations (2), (4) and (6) become:

$$\eta_a = -b_a \ln \left(1 - \frac{i}{i_{\text{la}}} \right) + b_a \ln(1 + \mu) \quad (\text{A.13})$$

$$\eta_c = -b_c \ln \left[1 - \frac{i}{i_{\text{lc}}} - \alpha \left(1 - \frac{i}{i_{\text{la}}} \right) \right] \quad (\text{A.14})$$

$$\eta_\Omega = \frac{d\eta_\Omega}{di} = 0 \quad (\text{A.15})$$

Differentiating as before, we obtain:

$$\frac{d\eta_a}{di} = \frac{0.5 + b_a}{i_{\text{la}}} \quad (\text{A.16})$$

$$\frac{d\eta_c}{di} = \left(\frac{0.5 + b_c}{1 - \alpha} \right) \left(\frac{i_{\text{la}} - \alpha i_{\text{lc}}}{i_{\text{lc}} i_{\text{la}}} \right) \quad (\text{A.17})$$

Neglecting anodic mass transport limitations as before, and substituting (A.17) into equation (A.3) for permeability limited conditions we obtain:

$$P_{\text{mx}} \approx \frac{0.25(1 - \alpha)i_{\text{lc}}i_{\text{la}}}{(0.5 + b_c)(i_{\text{la}} - \alpha i_{\text{lc}})} \quad (\text{A.18})$$

References

- [1] T. Schultz, S. Zhou, K. Sundmacher, Chem. Eng. Technol. 24 (2001) 1223–1233.
- [2] Y.M. Kim, K.W. Park, J.H. Choi, I.S. Park, Y.E. Sung, Electrochem. Commun. 5 (2003) 571–574.
- [3] P. Dimitrova, K.A. Friedrich, B. Vogt, U. Stimming, J. Electroanal. Chem. 532 (2002) 75–83.
- [4] W.C. Choi, J.D. Kim, S.I. Woo, J. Power Sources 96 (2001) 411–414.
- [5] S.P. Nunes, B. Ruffmann, E. Rikowski, S. Vetter, K. Richau, J. Membr. Sci. 203 (2002) 215–225.
- [6] V. Tricoli, F. Nannetti, Electrochim. Acta 48 (2003) 2625–2633.
- [7] B.S. Pivovar, Y. Wang, E.L. Cussler, J. Membr. Sci. 154 (1999) 155–162.
- [8] B. Libby, W.H. Smyrl, E.L. Cussler, AIChE J. 49 (2003) 991–1001.
- [9] G. Alberti, M. Casciola, Ann. Rev. Mater. Res. 33 (2003) 129–154.
- [10] D.H. Jung, S.Y. Cho, D.H. Peck, D.R. Shin, J.S. Kim, J. Power Sources 106 (2002) 173–177.
- [11] Y.I. Park, J.D. Kim, M. Nagai, J. Mater. Sci. Lett. 19 (2000) 1621–1623.
- [12] T. Yamaguchi, F. Miyata, S. Nakao, J. Membr. Sci. 214 (2003) 283–292.
- [13] B. Ruffmann, H. Silva, B. Schulte, S.P. Nunes, Solid State Ionics 162 (2003) 269–275.
- [14] D.H. Jung, Y.B. Myoung, S.Y. Cho, D.R. Shin, D.H. Peck, Int. J. Hydrogen Energy 26 (2001) 1263–1269.

- [15] H.Y. Chang, C.W. Lin, *J. Membr. Sci.* 218 (2003) 295–306.
- [16] Y. Woo, S.Y. Oh, Y.S. Kang, B. Jung, *J. Membr. Sci.* 220 (2003) 31–45.
- [17] J.T. Wang, J.S. Wainright, R.F. Savinell, M. Litt, *J. Appl. Electrochem.* 26 (1996) 751–756.
- [18] J.S. Wainright, J.T. Wang, D. Weng, R.F. Savinell, M. Litt, *J. Electrochem. Soc.* 142 (1995) L121–L123.
- [19] M.B. Berry, B.E. Libby, K. Rose, K.-H. Hass, R.W. Thompson, *Microporous Mesoporous Mater.* 39 (2000) 205–217.
- [20] D.H. Jung, S.Y. Cho, D.H. Peck, D.R. Shin, J.S. Kim, *J. Power Sources* 118 (2003) 205–211.
- [21] B. Libby, W.H. Smyrl, E.L. Cussler, *Electrochem. Solid State Lett.* 4 (2001) A197–A199.
- [22] D.W. Breck, *Zeolite Molecular Sieves: Structure, Chemistry, and Use*, Wiley/Interscience, New York, 1974.
- [23] J.H. Chang, J.Y. Park, G.G. Park, C.S. Kim, O.O. Park, *J. Power Sources* 124 (2003) 18–25.
- [24] Z. Poltarzewski, W. Wieczorek, J. Przulski, V. Antonucci, *Solid State Ionics* 119 (1999) 301–304.
- [25] A.S. Aricò, V. Baglio, A. Di Blasi, V. Antonucci, *Electrochem. Commun.* 5 (2003) 862–866.
- [26] E. Peled, T. Duvdevani, A. Melman, *Electrochem. Solid State Lett.* 1 (1998) 210–211.
- [27] E. Peled, T. Duvdevani, A. Aharon, A. Melman, *Electrochem. Solid State Lett.* 3 (2000) 525–528.
- [28] D. Satolli, M.A. Navarra, S. Panero, B. Scrosati, D. Ostrovski, P. Jacobsson, I. Albinsson, B.-E. Mellander, *J. Electrochem. Soc.* 150 (2003) A267–A273.
- [29] M.A. Navarra, S. Materazzi, S. Panero, B. Scrosati, *J. Electrochem. Soc.* 150 (2003) A1528–A1532.
- [30] A.A. Kulikovskiy, *Electrochem. Commun.* 4 (2002) 939–946.
- [31] A.A. Kulikovskiy, *Electrochem. Commun.* 5 (2003) 1030–1036.
- [32] K. Sundmacher, T. Schultz, S. Zhou, K. Scott, M. Ginkel, E.D. Gilles, *Chem. Eng. Sci.* 56 (2001) 333–341.
- [33] K. Scott, W. Taama, J. Cruickshank, *J. Power Sources* 65 (1997) 159–171.
- [34] K.T. Jeng, C.W. Chen, *J. Power Sources* 112 (2002) 367–375.
- [35] A. Parthasarathy, S. Srinivasan, A.J. Appleby, C.R. Martin, *J. Electrochem. Soc.* 139 (1992) 2530–2537.
- [36] X. Ren, T.E. Springer, S. Gottesfeld, *J. Electrochem. Soc.* 147 (2000) 92–98.
- [37] S. Gottesfeld, M.S. Wilson, in: T. Osaka, M. Datta (Eds.), *Energy Storage Systems for Electronics Devices*, Gordon and Breach Science Publishers, Singapore, 2000, p. 487.
- [38] Z.H. Wang, C.Y. Wang, *J. Electrochem. Soc.* 150 (2003) A508–A519.
- [39] K. Sundmacher, K. Scott, *Chem. Eng. Sci.* 54 (1999) 2927–2936.
- [40] I.S. Afanassyev, N.K. Moroz, *Solid State Ionics* 160 (2003) 125–129.
- [41] M. Doyle, S.K. Choi, G. Proulx, *J. Electrochem. Soc.* 147 (2000) 34–37.